



EFFECT OF STRONTIUM ION ON LUMINESCENCE PROPERTIES OF Eu^{3+} AND Ce^{3+} ACTIVATED $\text{K}_2\text{CASR}(\text{SO}_4)_3$ PHOSPHOR

P.C. Dhabale, M.S. Mendhe, P.P. Bhure, S.P. Puppalwar*

Department of Physics, Kamla Nehru Mahavidyalaya, Nagpur 440024, India

ABSTRACT

Eu^{3+} and Ce^{3+} activated $\text{K}_2\text{CaSr}(\text{SO}_4)_3$ has been synthesized by wet chemical method. X-Ray diffraction and SEM micrographs studies were used to determine their phase formation, purity and morphology. Photoluminescence excitation spectrum of Ce^{3+} activated $\text{K}_2\text{CaSr}(\text{SO}_4)_3$ (KCSS) show that the phosphor can be efficiently excited by UV light around 270 nm to realize emission in the near UV range due to the 5d–4f transition of Ce^{3+} ions which is applicable for scintillation purpose. Whereas Eu^{3+} activated $\text{K}_2\text{CaSr}(\text{SO}_4)_3$ phosphor emits orange/red emission at 594 and 617 nm respectively. Eu^{3+} ion is a promising candidate for solid state lighting. The change in concentration of Sr^{2+} in the host affect the photoluminescence characteristics of $\text{K}_2\text{Ca}_{(2-x)}\text{Sr}_x(\text{SO}_4)_3$. The newly synthesized phosphors by low cost and easy technique may be useful for solid state lighting application.

Keywords: $\text{K}_2\text{CaSr}(\text{SO}_4)_3$, XRD, SEM, Photoluminescence, Rare earths

1. Introduction

Sulphates are important family of luminescent materials and have attracted intense attention. In particular, researchers have concentrated on the sulphate series of phosphors with an ABSO_4 structure, where A is a monovalent cation (Li^+ , Na^+ , K^+ , Rb^+ , and Cs^+) and B is a divalent cation (Mg^{2+} , Ca^{2+} , Sr^{2+} , and Ba^{2+}) due to their large band gap, along with the high absorption of SO_4^{3-} in UV region, their moderate phonon energy, high thermal and chemical stability, and exceptional optical damage threshold. The rare earth (RE) activated inorganic compounds have attracted the attention due to their potential

applications, e.g., flat panel displays [1], long-lasting phosphorescent materials [2], thermoluminescence dosimeters [3], electroluminescence devices [4], white light-emitting diodes [5], scintillators [6] and non-destructive test [7]. For example, the luminescence spectra of Eu^{3+} ion doped in many hosts have been intensively investigated, including aluminates [8], sulphides [9], borates [10], phosphates [11], etc. The luminescent properties of Ce^{3+} doped compounds have been of considerable interest in recent years [12, 13]. Ce^{3+} has a very simple electron configuration, there is only one electron in the 4f shell and it is an excellent system for studying the behaviour of one-electron 4f and 5d states in different environments [14]. Ce^{3+} exhibits host dependent 4f–5d absorption and 5d–4f emission due to the strong interaction between its 5d states and the crystal lattice. The ground 4f1 electronic configuration of Ce^{3+} is split by a spin–orbit interaction into two sublevels, $2F_{5/2}$ and $2F_{7/2}$, with an energy interval of $\sim 2000 \text{ cm}^{-1}$ [15,16]. The 4f–5d transitions are electric dipole allowed transitions and, because there is only one single electron in the 5d configuration, repulsion between 5d electrons is absent [17]. Rare-earth elements have a unique electronic configuration of the 4f, and the luminescent properties of rare earth are due to the transition of 4f electrons of rare earth between different energy levels. Investigations on phosphors, especially, rare earth phosphors for white LED are very active [18]. Their chemical composition, degree of structural disorder, defects and the presence of dopants/impurities have notable influence on the electronic and optical properties of luminescent materials.

In this study, Eu^{3+} and Ce^{3+} activated $\text{K}_2\text{CaSr}(\text{SO}_4)_3$ an efficient phosphor has been

synthesized by wet chemical method. X-Ray diffraction and SEM micrographs studies were used to determine their phase formation, purity and morphology. The change in concentration of Sr^{2+} ion in the host, affect the PL characteristics of $\text{K}_2\text{Ca}_{(2-x)}\text{Sr}_x(\text{SO}_4)_3$. Therefore, newly synthesized phosphors by low cost and easy technique may be useful for scintillation purpose and solid state lighting application.

2. Experimental

2.1 Samples preparation

$\text{K}_2\text{CaSr}(\text{SO}_4)_3$ phosphors were prepared by the wet chemical method. The starting materials were analytical grade K_2SO_4 , CaSO_4 , SrSO_4 and rare earth oxide Eu_2O_3 , $\text{NH}_4\text{Ce}(\text{NO}_3)_3$ (AR grade of 99.99% purity – LOBA). Stoichiometric amounts of K_2SO_4 , CaSO_4 and SrSO_4 were taken in separate beakers and dissolved in double distilled de-ionized water so that their transparent solutions were obtained. These transparent solutions were then mixed together. Eu_2O_3 (AR grade of 99.99% purity – E. Merck) dissolved in dilute nitric acid in a separate beaker was also added to $\text{K}_2\text{CaSr}(\text{SO}_4)_3$ solution. The concentrations of Eu was taken $x = 0.5, 1, 1.5, 2$ and 2.5 mol %. The compound $\text{K}_2\text{CaSr}(\text{SO}_4)_3$: Eu in its powder form was obtained by evaporating with constant stirring continuously at 80°C about 8 hrs. The dried sample was then calcined at 700°C for 2 hr in carbon atmosphere, where the redox reaction occurs. The resultant powder was crushed to fine particles in a mortar pestle. The same procedure was used to prepare Ce doped $\text{K}_2\text{CaSr}(\text{SO}_4)_3$. These powders were used as a phosphor in further study.

2.2 Characterizations

The XRD technique was used in order to identify the product and check their

crystallinity. The phase composition and phase structure were measured by X-ray diffraction (XRD) pattern using a PAN-analytical diffractometer with Cu $\text{K}\alpha$ radiation ($\lambda=1.5405$ AU) operating at 40Kv, 30mA. The XRD data were collected in a 2θ range from 10 to 80° , with the continuous scan mode. The morphology and microstructure were characterized with JEOL, JSM-6360LV SEM environmental scanning electron microscope (SEM). The photoluminescence excitation and emission spectra were measured at room temperature by using a RF-5301PC SHIMADZU Spectrofluorophotometer equipped with a 150W Xenon lamp as the excitation source.

3. Results & Discussion

3.1 Phase purity and Morphology

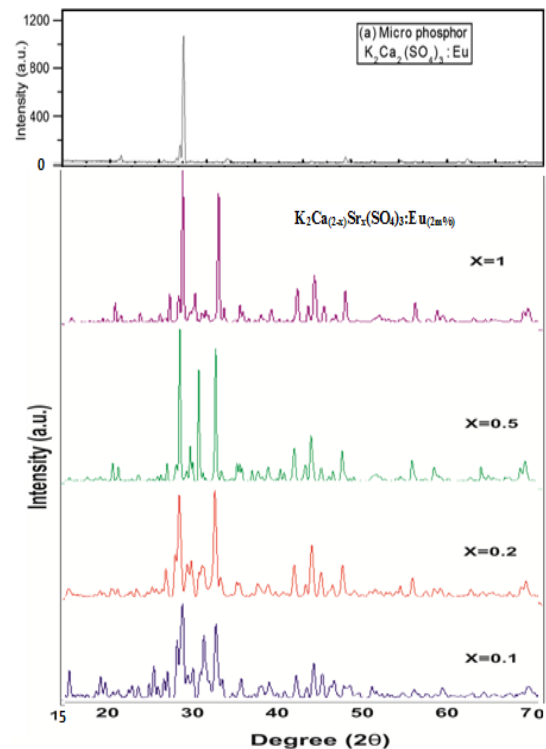


Fig. 1 XRD pattern of $\text{K}_2\text{Ca}_{2-x}\text{Sr}_x(\text{SO}_4)_3$ with different contents (x) of Sr.

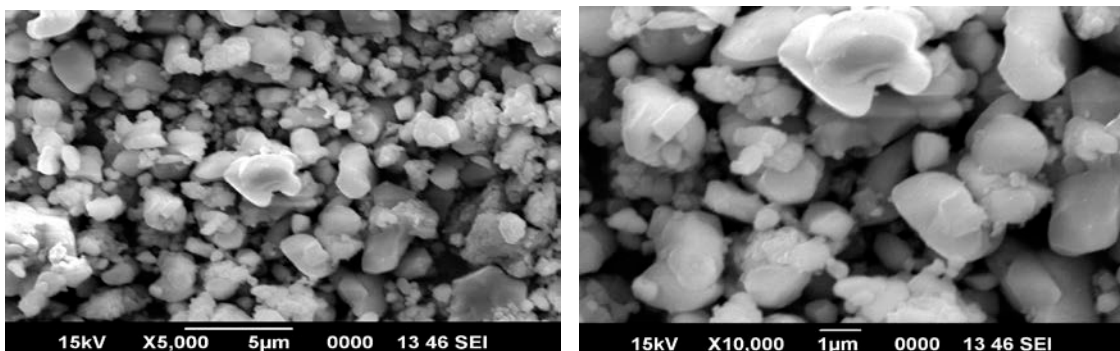


Fig. 2 SEM images of $\text{K}_2\text{CaSr}(\text{SO}_4)_3$ phosphor

X-ray diffraction pattern were recorded on Philips P Analytical X'Pert Pro diffractometer. The prepared samples, which were characterized for their phase purity and crystallinity at a scanning step of 0.01° , continue time 20 s, in the 2θ range $10\text{--}70^\circ$. Fig. 1 shows XRD pattern of $\text{K}_2\text{Ca}_{2-x}\text{Sr}_x(\text{SO}_4)_3$ phosphor for different (x) contents of Sr. The results for all samples with different content of Sr^{2+} ions are similar. No other phase or impurity can be detected, indicating that there is no significant effect of different content of Sr^{2+} ions other than intensity, on the $\text{K}_2\text{CaSr}(\text{SO}_4)_3$

host without inducing significant changes in the crystal structure. It was first synthesized by us. The detailed structure data will be published elsewhere. In literature there is no standard JCPDS file for XRD pattern of $\text{K}_2\text{CaSr}(\text{SO}_4)_3$ phosphor for comparison. SEM micrograph images of $\text{K}_2\text{CaSr}(\text{SO}_4)_3$ phosphors are shown in Fig. 2. The images show the particles are polycrystalline with some agglomeration. The crystallites have adhered with each other to form globular clusters of irregular size and shapes. The average size of the crystallites is found to be in the range of $1\text{--}2\ \mu\text{m}$.

3.2 PL properties of KCSS : Eu^{3+}

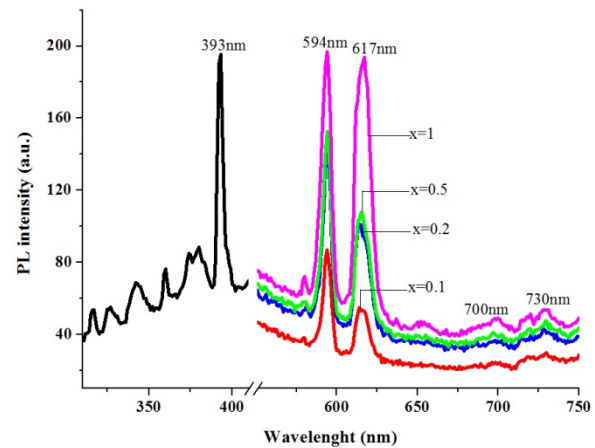
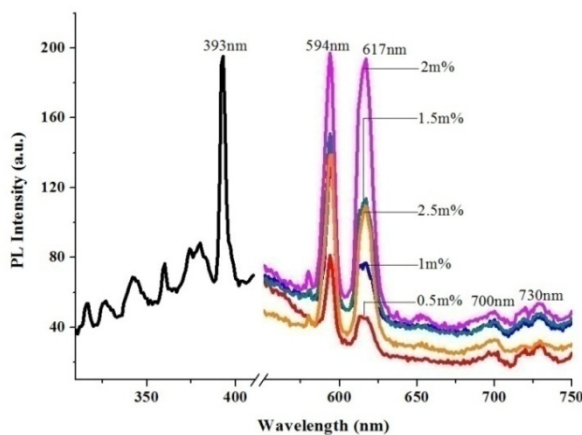


Fig.3. PL spectra of KCSS: $x\text{Eu}^{3+}$ phosphor monitored at 393nm excitation. Fig. 4 PL spectra of $\text{K}_2\text{Ca}_{(2-x)}\text{Sr}_x(\text{SO}_4)_3:\text{Eu}_{(2m\%)}$ phosphor monitored at 393 nm excitation.

Photoluminescence excitation and emission spectra of $\text{KCSS}:\text{Eu}^{3+}$ are shown in Fig.3. The excitation spectrum consists some sharp lines in the region $320\text{--}420\ \text{nm}$ due to the $f\text{--}f$ transitions within Eu^{3+} , $4f^6$ electron configuration with ${}^7\text{F}_0 - {}^5\text{L}_6$ (393 nm) transition as the most prominent line. The emission spectra are obtained by excitation of Eu^{3+} at 393 nm. The emission spectra of $\text{KCSS}:\text{xEu}^{3+}$ consists of a series of sharp lines in the region $550\text{--}750\ \text{nm}$. The lines belong to transitions between the energy levels of the $4f^6$ configuration of Eu^{3+} ion. The emission spectra exhibit two main regions: the more intense one includes maxima at 594 nm (${}^5\text{D}_0\text{--}{}^7\text{F}_1$) and at 617 nm (${}^5\text{D}_0\text{--}{}^7\text{F}_2$) (Fig.3). Apart from these prominent peaks, we could also observe other weak emission peaks centered at 654, 700 and 730 nm corresponding to (${}^5\text{D}_0 \rightarrow {}^7\text{F}_3$), (${}^5\text{D}_0 \rightarrow {}^7\text{F}_4$) and (${}^5\text{D}_0 \rightarrow {}^7\text{F}_5$) transitions, respectively. When Eu^{3+} ion is put into the Sr^{2+} site, which is coordinated by six

O^{2-} ions, the splitting of energy levels by crystal field would change with the position of Eu^{3+} ion in the crystal lattice. Eu^{3+} emission usually occurs from ${}^5\text{D}_0 \rightarrow {}^7\text{F}_j$ transitions. The ${}^5\text{D}_0 \rightarrow {}^7\text{F}_1$ transition is allowed as magnetic dipole transition. This is the only transition when Eu^{3+} is situated at a site coinciding with a centre of symmetry. ${}^5\text{D}_0 \rightarrow {}^7\text{F}_2$ allowed as forced electric dipole transition and is induced when Eu^{3+} is situated at a site which lacks the inversion symmetry. The transition ${}^7\text{F}_1$ state is stronger than that of the transition to ${}^7\text{F}_2$ state. The emission in the vicinity of 600 nm is due to the magnetic dipole transition ${}^5\text{D}_0 \rightarrow {}^7\text{F}_1$, which is insensitive to the site symmetry. The emission around 610–630 nm is due to the electric dipole transition of ${}^5\text{D}_0 \rightarrow {}^7\text{F}_2$, induced by the lack of inversion symmetry at the Eu^{3+} site, is less stronger than that of the transition to the ${}^7\text{F}_1$ state. Fig.3 shows the emission spectra of $\text{KCSS}:\text{xEu}^{3+}$ for various concentration of Eu^{3+} .

It is found that the emission intensity reaches maximum at $x = 2\text{mol}\%$ and then decreases with more doping concentration of Eu^{3+} . Addition of Sr^{2+} ion in the host affects the photoluminescence characteristics with same profile. The emission spectra of $\text{K}_2\text{Ca}_{2-x}\text{Sr}_x(\text{SO}_4)_3:\text{Eu}^{3+}$ ($2\text{mol}\%$) for various concentration of Sr^{2+} ion is shown in Fig.4. It is

found that the emission intensity increases with increasing Sr^{2+} content and reaches a maximum at $x = 1$. $\text{KCSS}:\text{Eu}^{3+}$ material is proposed as an orange-red phosphor and can be used in lamp industry. Fig. 5 shows that change in intensity with variation of Sr^{2+} content. Sr^{2+} and Eu^{3+} ions in $\text{K}_2\text{Ca}_{(2-x)}\text{Sr}_x(\text{SO}_4)_3:\text{Eu}_{(2\text{m}\%)}$ have same profile, which is also shown in Table 1.

3.3PL properties of $\text{KCSS}:\text{Ce}^{3+}$

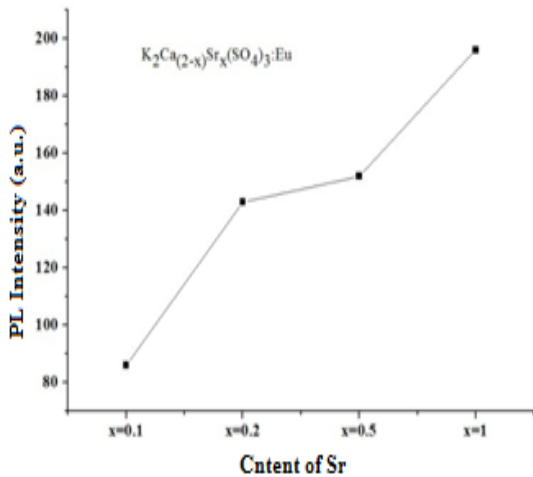


Fig. 5 Change in PL intensity with variation of Sr^{2+} content in phosphor monitored at $\text{K}_2\text{Ca}_{(2-x)}\text{Sr}_x(\text{SO}_4)_3:\text{Eu}_{(2\text{m}\%)}$.

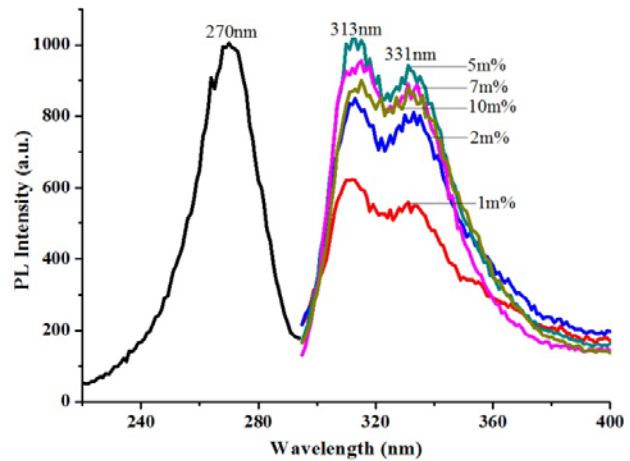


Fig. 6 PL spectra of $\text{K}_2\text{CaSr}(\text{SO}_4)_3:\text{xCe}^{3+}$ 270nm excitation. ($\lambda_{\text{emi}}=313\text{nm}$)

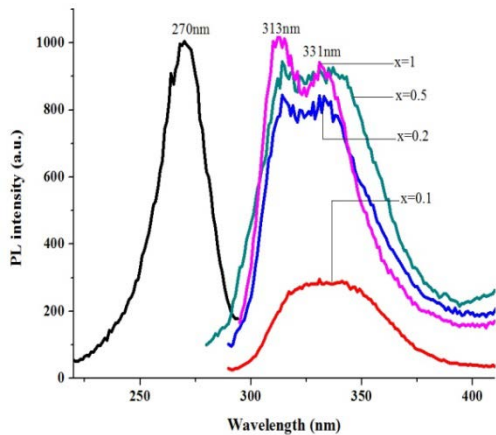


Fig. 7 PL spectra of $\text{K}_2\text{Ca}_{(2-x)}\text{Sr}_x(\text{SO}_4)_3:\text{Ce}_{(5\text{m}\%)}$ showing 270nm excitation. ($\lambda_{\text{emi}}=313\text{nm}$)

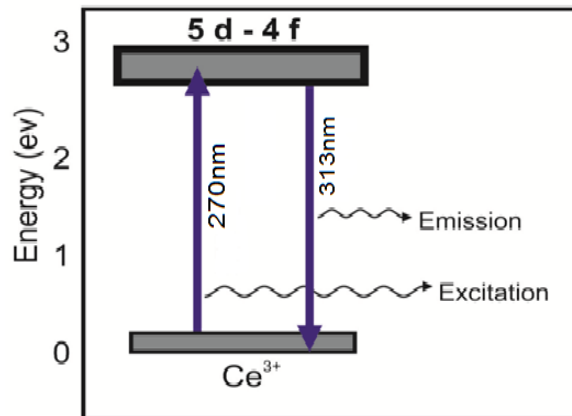


Fig. 8. Schematic energy level diagram $\text{K}_2\text{CaSr}(\text{SO}_4)_3:\text{Ce}^{3+}$

The ultraviolet (UV) excitation spectrum shows a strong principal centre at 270nm. This could be assigned to the $4f \rightarrow 5d$ transition of Ce^{3+} ions in solids is parity allowed electric dipole transition ($f - d$) and has large oscillator strength and produces efficient broadband luminescence. Where $4f$ is the lowest excited charge transfer state of the Ce^{3+} ion and $5d$ is the molecular orbital of the surrounding ligand. The emission spectra of $\text{KCSS}:\text{Ce}^{3+}$ for different concentrations of Ce^{3+} excited at 270nm is shown in Fig.6. Two strong resolved

peaks in emission spectra are observed at 311 and 331 nm, which are assigned to the $5d-4f$ transition of Ce^{3+} ions. The double humped emission spectrum is characteristic of Ce^{3+} and could be attributed to $5d-4f$ (${}^2F_{5/2}$, ${}^2F_{7/2}$) transitions. The excitation to this band is observed around 270nm. The observed variations of PL emission intensities may be cross relaxation between Ce^{3+} ions in the case of heavy concentration of Ce^{3+} . The emission of the Ce^{3+} doped sample is dominated by the ${}^4f_0 \rightarrow {}^5d_1 \rightarrow {}^4f_1$ (${}^2F_{5/2}$) transition of Ce^{3+} (313nm),

whereas the host excitation emission is quenched. In the excitation spectra, there is a broad absorption band between 240 and 290nm on the excitation spectrum of Ce³⁺ doped KCSS. Based on the fact that the Ce³⁺ 5d manifold undergoes an energetic depression on the basis of the nephelauxetic effect and a large splitting due to the crystal field. From the measured fluorescence spectra of Ce³⁺, it is clear that band corresponds to the transitions 5d-4f. The fluorescence intensity is the maximum for 5mol% of Ce concentration, beyond which, the fluorescence intensity tends to quench. It is also noticed that the peak positions of the emission bands have not

changed. These phosphors are emitting in the UV region. In Fig. 7, PL of a series of KCSS: Ce³⁺ (0.5m %) sample with varying values of Sr²⁺ (x = 0.1 ≤ x ≤ 1) is shown and effect of doped Ce³⁺ concentration on the emission intensity was investigated. With increasing (x) content of Sr²⁺, the intensity peak increased and maximum intensity was observed for x = 1. No quenching could be observed in Sr²⁺ content range. It shows that the PL characteristics of the material is better for x = 1 than other values of x in the sample. The results suggest that KCSS: Ce³⁺ may serve as a promising material for use as a UV emitting lamp phosphor.

Table 1.

Phosphor	Emission wavelength in nm, ($\lambda_{ext} = 393nm$)	PL Intensity (a.u.)
K ₂ Ca _(2-x) Sr _x (SO ₄) ₃ :Eu(2m%), _{x=0.1}	594, 614, 700, 730	86, 54, 24, 29
K ₂ Ca _(2-x) Sr _x (SO ₄) ₃ :Eu(2m%), _{x=0.2}	594, 614, 700, 730	143, 101, 36, 43
K ₂ Ca _(2-x) Sr _x (SO ₄) ₃ :Eu(2m%), _{x=0.5}	594, 615, 700, 730	152, 107, 39, 47
K ₂ Ca _(2-x) Sr _x (SO ₄) ₃ :Eu(2m%), _{x=1}	594, 617, 700, 730	196, 193, 49, 53

Table 2.

Phosphor	Emission wavelength in nm ($\lambda_{ext} = 270nm$)	PL Intensity(a.u.)
K ₂ Ca _(2-x) Sr _x (SO ₄) ₃ :Ce(5m%), _{x=0.1}	317, 331	259, 294
K ₂ Ca _(2-x) Sr _x (SO ₄) ₃ :Ce(5m%), _{x=0.2}	317, 331	844, 841
K ₂ Ca _(2-x) Sr _x (SO ₄) ₃ :Ce(5m%), _{x=0.5}	314, 331	944, 922
K ₂ Ca _(2-x) Sr _x (SO ₄) ₃ :Ce(5m%), _{x=1}	313, 331	1015, 942

4. Conclusion

Polycrystalline Eu³⁺ and Ce³⁺ doped K₂CaSr(SO₄)₃ sulfate phosphors were successfully prepared via wet chemical synthesis method. The structural properties of these phosphors were investigated by XRD. Surface morphology was determined by SEM and it shows good connectivity with grains including some agglomerates and defect in the

prepared phosphor. The samples are excited by 393nm, and show two strong emission peaks at 594 and 617 nm corresponding to the ⁵D₀→⁷F₁ and ⁵D₀→⁷F₂ transition of Eu³⁺. The results reveal that Na₂Ca_{2-x}Mg_x(SO₄)₃ is the low cost and better orange-red phosphor. PL emission spectra of Ce³⁺ doped KCSS prepared phosphors were observed in the UV region. Upon 270 nm excitation, it displayed efficient

broadband emission in the UV region with maximum intensity at 313 nm. The optical properties of these phosphors led to the conclusion that they may serve as promising materials for use as lamp phosphors in the UV region.

Acknowledgements

Author SPP is thankful to management of the Institution KNM, Nagpur for providing useful facilities of the instrumentation, SHIMADZU Spectrofluorophotometer (RF-5301 PC) to carry out this work.

REFERENCES

- [1] Yokota H, Yoshida M, Ishibashi H, Yano T., Yamamoto H., Kikkawa S. Concentration effect of Cerium in $(Y_{0.9-x}Gd_{0.1}Ce_x)_2SiO_5$ blue phosphor. *J. Alloys Compd.* 2010; 495; 162–166.
- [2] Xiao L, Xiao Q, Liu Y, Ai P, Li Y, Wang H, A transparent surface-crystallized Eu^{2+}, Dy^{3+} co-doped strontium aluminate long lasting phosphorescent glass-ceramic. *J. Alloys Compd.* 2010; 495; 72–75.
- [3] Vij A, Lochab SP, Singh S, Kumar R, Singh N. TL study of UV irradiated Ce doped SrS nanostructures. *J. Alloys Compd.* 2009; 486; 554–558.
- [4] Yang SH, Lial YJ, Cheng NJ, Ling YH, Preparation and characterization of yellow ZnS:Mn,Ce phosphor. *J. Alloys Compd.* 2010; 489; 689–693.
- [5] Zhang XM, Li L, Seo HJ, Luminescence and energy transfer in Eu^{2+}, Mn^{2+} co-doped $Li_4SrCa(SiO_4)_2$ for white light-emitting-diode. *Phys. Lett. A* 2009; 373; 3486–3489.
- [6] Feng H, Ding D, Li H, Lu S, Pan S, Chen X, Ren G, Growth and Luminescence characteristics of Cerium doped yttrium pyrosilicate single crystal. *J. Alloys Compd.* 2010; 489; 645–649.
- [7] Yang F, Pan SK, Ding DZ, Chen XF, Lu S, Zhang WD, Ren GH, Growth and optical properties of the Ce doped $Li_6Gd(BO_3)_3$ crystal grown by the modified Bridgeman method, *J. Alloys Compd.* 2009; 484; 837–840.
- [8] Cao D, Zhao G, Chen J, Dong Q, Ding Y, Cheng Y, Effect of growth atmosphere and annealing on luminescence efficiency of YAP:Ce crystal. *J. Alloys Compd.* 2010; 489; 515–518.
- [9] Kumar V, Pitale SS, Mishra V, Nagpure IM, Biggs MM, Ntwaeaborwa OM, Swart HC, Luminescence investigation of Ce^{3+} doped CaS nanophosphor. *J. Alloys Compd.* 2010; 492; L8–L12.
- [10] Jiang LH, Zhang YL, Li CY, Hao JQ, Su Q, Synthesis PL, TL and dosimetry properties of novel phosphor $KSr_4(BO_3)_3:Ce$. *J. Alloys Compd.* 2009; 482; 313–316.
- [11] Puppalarwar SP, S.J. Dhoble. Luminescent properties of $LiBaPO_4:M^{3+}$ phosphor for near-UV light-emitting diode (M=Eu and Dy), *J. Bio and Chem. Lumin.* DOI 10.1002/bio.2815 (2015).
- [12] Luo Y, Xia Z, Liu H, He Y. Synthesis and luminescence properties of blue-emitting phosphor $K_2Ca_2Si_2O_7:Ce^{3+}$. *Opt Mater* 2014; 36: 723–726.
- [13] Lijun L, Hongmei F, Yan T, Wanjun T. Novel blue-emitting phosphor $NaMg_4(PO_4)_3:Eu^{2+}, Ce^{3+}$ with energy transfer. *Opt Mater* 2011; 34; 175–8.
- [14] BrikMG, Ma C-G, Liang H, Ni H, Liu G. Theoretical analysis of optical spectra of Ce^{3+} in multi-sites host compounds. *J Lumin* 2014; 152; 203–5.
- [15] Bhojar P, Dhoble SJ. Electron–vibrational interaction in 5d state of Ce^{3+} ion in $(LiMg/Li_2Na/Li_3)BF_6$ phosphors. *Mater Chem Phys* 2013; 140: 104–7.
- [16] Brik MG, Avram NM. Electron–vibrational interaction in the 5d states of Ce^{3+} ions in halosulphate phosphors. *Mater ChemPhys* 2011; 128; 326–30.
- [17] Wang T, Xia Z, Xiang Q, Qin S, Liu Q. Relationship of 5d-level energies of Ce^{3+} with the structure and composition of nitride hosts. *J Lumin* 2015; 166: 106–10.
- [18] Shinde N, Dhoble NS, Gedam SC, Dhoble SJ. Photoluminescence enhancement in $Na_3SO_4Cl:X$ ($X=Ce^{3+}, Eu^{3+}$ or Dy^{3+}) material. *J. Bio and Chemi Luminescence* 30(2015) 898–903.